

# Formation of Iron(III) *meso*-Chloro-isoporphyrin as a Reactive Chlorinating Agent from Oxoiron(IV) Porphyrin $\pi$ -Cation Radical

Zhiqi Cong, Takuya Kurahashi, and Hiroshi Fujii\*

Institute for Molecular Science and Okazaki Institute for Integrative Bioscience, National Institutes of Natural Sciences, Myodaiji, Okazaki 444-8787, Japan

**S** Supporting Information

**ABSTRACT:** Iron(III) isoporphyrin, a tautomer of porphyrin with a saturated *meso* carbon, is one of the isoelectronic forms of oxoiron(IV) porphyrin  $\pi$ -cation radical, which is known as an important reactive intermediate of various heme enzymes. The isoporphyrin has been believed to be incapable of catalyzing oxygenation and oxidation reactions. Here, we report that an oxoiron(IV) porphyrin  $\pi$ -cation radical can be converted to iron(III) *meso*-chloro-isoporphyrin in the presence of trifluoroacetic acid and chloride ion. More importantly, this study shows the first evidence that iron(III) *meso*-chloro-isoporphyrin is an excellent reactive agent for chlorinating aromatic compounds and olefins. The results of this study suggest that the mechanism involves electrophilic chlorination of substrate with iron(III) *meso*-chloro-isoporphyrin.

Oxoiron(IV) porphyrin  $\pi$ -cation radicals are generally known to function as key reactive intermediates in a variety of oxidation reactions catalyzed by heme enzymes such as cytochrome P450.<sup>1</sup> The oxoiron(IV) porphyrin  $\pi$ -cation radical complex has several isoelectronic forms which are two oxidation state equivalents higher than the iron(III) porphyrin complex: for example, oxoiron(V) porphyrin,<sup>2</sup> iron(III) porphyrin *N*-oxide,<sup>3</sup> iron(III) porphyrin  $\pi$ -dication,<sup>4</sup> and iron(III) isoporphyrin complexes.<sup>5</sup> Isoporphyrins—tautomers of porphyrins with a saturated *meso* carbon—were originally postulated by Woodward,<sup>6</sup> and the first isoporphyrin–metal complex was reported by Dolphin et al.,<sup>7</sup> who prepared a zinc(II) 5'-methoxy-5,10,15,20-tetraphenylisoporphyrin complex by nucleophilic attack of methanol on zinc(II) 5,10,15,20-tetraphenylporphyrin  $\pi$ -dication complex. Since then, iron(III) isoporphyrin complexes, particularly *meso*-tetraaryl derivatives, have been synthesized chemically and electrochemically.<sup>5</sup> For example, an iron(III) isoporphyrin complex with a *tert*-butylperoxy group was prepared by reaction of iron(III) porphyrin complexes with *tert*-butyl hydroperoxide, a two-electron oxidant.<sup>5a</sup> The reaction of electron-rich iron(III) porphyrin with nitrogen dioxide also afforded an iron(III) isoporphyrin complex with hydroxide, and its structure was confirmed by X-ray crystallography.<sup>5b</sup> Moreover, an unstable iron(III) isoporphyrin with a pyridinium group was reported to be formed from an iron(III) porphyrin  $\pi$ -cation radical complex with pyridine.<sup>5c</sup> On the other hand, iron(III) isoporphyrins have been proposed to be formed in reactions of heme

enzymes.<sup>8–12</sup> The iron(III) isoporphyrin complex is two oxidation state equivalents higher than the iron(III) porphyrin complex. However, to our surprise, atom-transfer reactions of isoporphyrin complexes with substrates, such as oxygenation and halogenation reactions, have not been well studied.<sup>8</sup> In this study, we show that an oxoiron(IV) porphyrin  $\pi$ -cation radical complex can be converted to iron(III) *meso*-chloro-isoporphyrin complex in the presence of trifluoroacetic acid (TFA) and chloride ion. Formation of the isoporphyrin complex would be due to protonations of the oxo ligand of oxoiron(IV) porphyrin  $\pi$ -cation radical species. More importantly, this study shows that the iron(III) *meso*-chloro-isoporphyrin complex is a reactive reagent for chlorination of aromatic compounds and olefins.

(TPFP<sup>IV</sup>)Fe<sup>IV</sup>O(NO<sub>3</sub>) (TPFP = 5,10,15,20-tetrakis-(pentafluorophenyl)porphinato) was prepared by ozone oxidation of (TPFP)Fe<sup>III</sup>(NO<sub>3</sub>) in dichloromethane (DCM) at –90 °C.<sup>13</sup> Upon addition of 20 equiv of TFA and 2 equiv of tetra-*n*-butylammonium chloride (TBACl) in turn, (TPFP<sup>IV</sup>)Fe<sup>IV</sup>O(NO<sub>3</sub>) was quickly converted to a new compound, **1**, which exhibits Soret bands of decreased intensity at 359 and 411 nm and an intense absorption at 939 nm (Figure 1). The absorption spectral features of **1** are similar to those of isoporphyrin complexes.<sup>5,7,14</sup> The small peak at 630 nm and the shoulder peak around 503 nm suggest that (TPFP)Fe<sup>III</sup>(X), (X = NO<sub>3</sub> or Cl) is formed concomitantly as a minor byproduct. **1** is stable for hours at –90 °C but quickly decomposes to (TPFP)Fe<sup>III</sup>Cl at room temperature. **1** could be also prepared by oxidation in a mixture of (TPFP)Fe<sup>III</sup>(NO<sub>3</sub>), TBACl (2 equiv), and TFA (20 equiv) with ozone gas at –90 °C (Scheme 1 and Figure S1). A similar compound, **2**, is formed when a mixture of (TDBP)Fe<sup>III</sup>Cl (TDBP = 5,10,15,20-tetrakis(3',5'-di-*tert*-butylphenyl)porphinato), TBACl (2 equiv), and TFA (20 equiv) is oxidized by ozone gas in DCM at –40 °C (Figure S2). However, the ozone oxidation of (TDBP)Fe<sup>III</sup>Cl did not yield an oxoiron(IV) porphyrin  $\pi$ -cation radical species. **2** is stable for hours at –40 °C but almost completely decomposes to ferric porphyrin after 1 h at room temperature.

To confirm the isoporphyrin structures and iron oxidation states of **1** and **2**, we conducted NMR, EPR, and electrospray ionization mass spectrometry (ESI-MS) measurements. The formation and decomposition of **1** were monitored by <sup>2</sup>H NMR spectroscopy (Figure S3). The pyrrole-deuterated (TPFP<sup>IV</sup>)Fe<sup>IV</sup>O(NO<sub>3</sub>) has a deuterium NMR signal at –86.7 ppm at

Received: October 24, 2011

Published: February 29, 2012

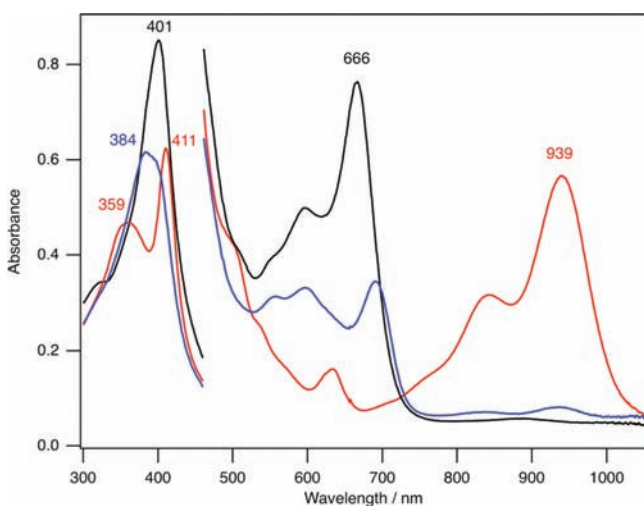
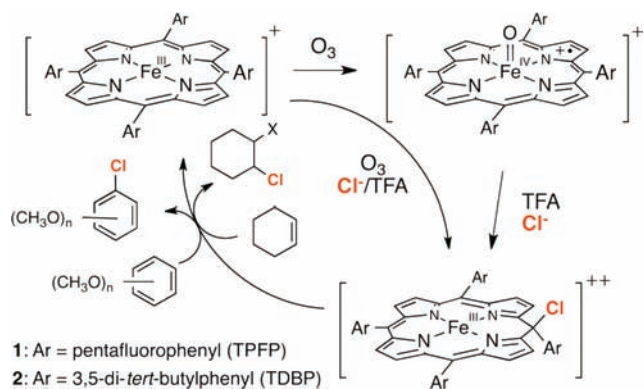


**Figure 1.** UV-visible absorption spectral change during the reaction of  $(\text{TPFP}^{+\bullet})\text{Fe}^{\text{IV}}\text{O}(\text{NO}_3)$  with TBACl and TFA in  $\text{CH}_2\text{Cl}_2$  at  $-90^\circ\text{C}$ . Black line,  $(\text{TPFP}^{+\bullet})\text{Fe}^{\text{IV}}\text{O}(\text{NO}_3)$ ; blue line, after addition of TFA (20 equiv); red line, after addition of TBACl (2 equiv). The spectra at 300–460 and 460–1050 nm were measured with sample concentrations of  $2.0 \times 10^{-4}\text{ M}$  in a 0.05 cm quartz cuvette and  $5.0 \times 10^{-4}\text{ M}$  in a 0.1 cm quartz cuvette, respectively.

**Scheme 1. Formation of Iron(III) *meso*-Chloro-isoporphyrin from Iron(III) Porphyrin and Its Chlorination Reactions (Anions Omitted for Clarity)**

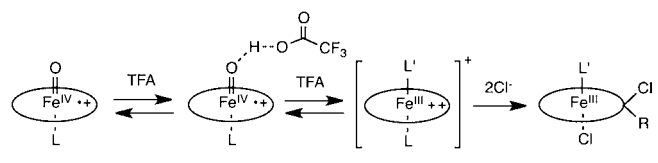


$-80^\circ\text{C}$ . The large upfield shift of the pyrrole signal is consistent with the  $a_{1u}$  porphyrin  $\pi$ -cation radical state as reported previously.<sup>15</sup> Upon addition of TFA (20 equiv) and TBACl (2 equiv) in turn at  $-80^\circ\text{C}$ , this  $^2\text{H}$  NMR signal disappears, and four new  $^2\text{H}$  NMR signals corresponding to **1** appear at  $\sim 110$ – $140$  ppm. The  $^2\text{H}$  NMR spectrum of **1** is consistent with the isoporphyrin structure.<sup>5a</sup> Upon increasing temperature to  $25^\circ\text{C}$ , the four signals of **1** disappear, and a new signal appears at 80 ppm, identical to the shift of the pyrrole  $\beta$ -deuterium signal of  $(\text{TPFP})\text{Fe}^{\text{III}}\text{Cl}$ . The same structural information was also obtained by  $^{19}\text{F}$  NMR spectroscopy (Figure S4). Similarly, the porphyrin structure of **2** was investigated by  $^1\text{H}$  NMR (Figure S5). As observed for **1**, **2** also has four  $^1\text{H}$  NMR signals of the pyrrole  $\beta$ -protons in the large downfield region of 90–110 ppm at  $-40^\circ\text{C}$  and decomposes to  $(\text{TDBP})\text{Fe}^{\text{III}}\text{Cl}$  upon warming up to  $25^\circ\text{C}$ . **1** and **2** have EPR signals at  $g = 6.0$  and  $2.0$  at 4 K (Figure S6), indicating ferric high-spin states. This is consistent with the large downfield shifts of the pyrrole  $\beta$ -proton (deuterium) signals of **1** and **2**. The structures of **1** and **2** were further studied by

ESI-MS at low temperature (Figures S7 and S8). The spectrum of **2** clearly exhibits a major ESI-MS peak at  $m/z$  1186.82 and an isotope pattern fully consistent with the ion  $[\text{C}_{76}\text{H}_{92}\text{N}_4\text{FeCl}_2]^+$ . This formula is identical to that of chloroiron(III) *meso*-chloroisoporphyrin cation (see Scheme 1). On the other hand, a strong ESI-MS peak with an isotope pattern consistent with an iron complex was detected at  $m/z$  1078.86 for **1**. The MS number and isotope pattern are consistent with the ion  $[\text{C}_{44}\text{H}_8\text{N}_4\text{F}_{20}\text{FeOCl}]^+$ . One of the possible structures for this ion formula is oxoiron(IV) *meso*-chloro-isoporphyrin cation or iron(IV) hypochlorite, which is one oxidation equivalent higher than **1** and  $(\text{TPFP}^{+\bullet})\text{Fe}^{\text{IV}}\text{O}(\text{NO}_3)$ . This ion may be produced by oxidation of **1** in the ionization process. Although the origin of the ESI-MS peak of **1** is not clear, the spectroscopic data shown here are consistent with iron(III) *meso*-chloroisoporphyrin structure.

The addition of TFA is essential to produce **1**. Previously, Watanabe et al. demonstrated the formation of a porphyrin  $\pi$ -dication from iron(III) porphyrin *N*-oxide complex with TFA.<sup>4</sup> It was proposed that iron(III) porphyrin  $\pi$ -dication is formed by protonation of the oxygen atom of the porphyrin *N*-oxide with TFA, followed by dissociation of a water molecule. In this study, TFA also functions as proton donor and protonates the oxo ligand of  $(\text{TPFP}^{+\bullet})\text{Fe}^{\text{IV}}\text{O}(\text{NO}_3)$ . In fact, **1** is formed even when hydrochloric acid is used instead of TFA, but **1** could not be formed with acetic acid. When TFA is titrated into a solution of  $(\text{TPFP}^{+\bullet})\text{Fe}^{\text{IV}}\text{O}(\text{NO}_3)$ ,  $(\text{TPFP}^{+\bullet})\text{Fe}^{\text{IV}}\text{O}(\text{NO}_3)$  is converted to a new species, and an isosbestic point is present until 1.4 equiv of TFA is added (Figure S9). Further addition of TFA produces the spectrum shown in Figure 1 (blue line). When TBACl is added after addition of 2 equiv of TFA, only a small amount of **1** is produced (Figure S10). The featureless absorption spectrum after addition of 20 equiv of TFA is consistent with iron(III) porphyrin  $\pi$ -dication. The Soret band at 384 nm rules out the formation of porphyrin *N*-substituted compounds, which have Soret bands at  $\sim 440$  nm.<sup>3b</sup> After addition of 20 equiv of TFA, the  $^2\text{H}$  NMR spectrum also exhibits NMR signals at  $\sim 120$  ppm, indicating the formation of ferric high-spin species (Figure S11).<sup>4</sup> Therefore, **1** appears to be produced from an oxoiron(IV) porphyrin  $\pi$ -cation radical via iron(III) porphyrin  $\pi$ -dication species (Scheme 2). The

**Scheme 2. Formation of **1** via the Iron(III) Porphyrin  $\pi$ -Dication Complex with Protonation of the Oxo Ligand**



protonation of the oxo ligand stabilizes the iron d-orbitals, resulting in formation of a porphyrin  $\pi$ -dication by intramolecular electron transfer from the porphyrin  $\pi$ -cation radical to the iron center.

To examine the chlorinating ability of **1** and **2**, we conducted chlorination reactions of various organic compounds. **1** was mixed with 50 equiv of 1,3,5-trimethoxybenzene at  $-90^\circ\text{C}$ . After being stirred for 3 min, the reaction mixture was allowed to warm to room temperature. The absorption spectrum of the final reaction solution was almost identical to that of  $(\text{TPFP})\text{Fe}^{\text{III}}\text{Cl}$ . The formation of  $(\text{TPFP})\text{Fe}^{\text{III}}\text{Cl}$  from the reaction was further confirmed by  $^1\text{H}$  NMR and EPR

measurements. After completion of the reaction at room temperature, the reaction product was analyzed by GC-MS. As shown in Figure 2, **1** is used to chlorinate 1,3,5-trimethoxy-

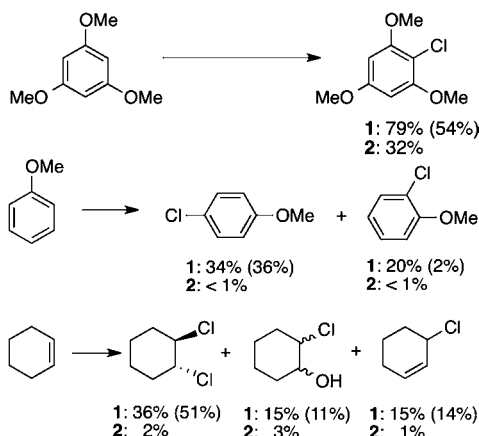


**Figure 2.** Chlorination of organic substrates by isoporphyrins **1** and **2**. The yields are based on the starting ferric porphyrins. The numbers in the parentheses show product yields obtained using a chlorinating agent formed from the reaction of **1** with 50 equiv of TBACl. The blank experiments, (TPFP)Fe<sup>III</sup>(NO<sub>3</sub>) in the presence of TBACl (2 equiv) and TFA (20 equiv), did not give significant amount of chlorination products (<1–2%).

ylbenzene to obtain 1-chloro-2,4,6-trimethoxybenzene in 79% yield. No other products, such as 1-chloromethoxy-3,5-dimethoxybenzene (a main product of a reaction with chlorine radical), are detected.<sup>16</sup> The chlorination reactions of anisole and cyclohexene were also examined under the same conditions. As shown in Figure 2, anisole is chlorinated by **1** to form 4-chloroanisole and 2-chloroanisole in 34% and 20% yields, respectively. A ratio (1.7) of the *para* and *ortho* isomers formed by **1** was close to those formed by CPO (**1.9**) and hypochlorous acid under acidic aqueous conditions (**1.8**),<sup>16</sup> but different from that (~10) by (TPFP<sup>+</sup>)Fe<sup>IV</sup>O(NO<sub>3</sub>).<sup>17</sup> The chlorination of the methoxy group of anisole was also not observed. Cyclohexene was chlorinated by **1** to form *trans*-1,2-dichlorocyclohexane (36%) as a major product, together with 2-chlorocyclohexanol (15%) and 3-chlorocyclohexene (15%). 4-Chlorocyclohexene and *cis*-1,2-dichlorocyclohexane, possible free-radical chlorination products, were not detected. On the other hand, **1** cannot chlorinate toluene. Similarly, the chlorination reaction of **2** was also examined. **2** chlorinates 1,3,5-trimethoxybenzene to give 1-chloro-2,4,6-trimethoxybenzene in a 32% yield, but is not active with respect to chlorination of anisole and cyclohexene. The chlorination reactivity of **1** is higher than that of **2**. This is probably due to the electron-withdrawing effect of the pentafluorophenyl group of **1**.

To reveal the chlorination mechanism, we conducted a kinetic study of the chlorination reaction of **1** by absorption spectroscopy at –40 °C (Figure S12). The absorption at 939 nm of **1** slightly decreases in intensity immediately upon addition of excess 1,3,5-trimethoxybenzene, and then the absorption spectrum changes to the spectrum of (TPFP)Fe<sup>III</sup>Cl with clear isosbestic points. The initial reaction process is too fast to estimate the reaction rate constant by absorption spectroscopy at –40 °C. The time course for the second reaction process can be fitted with first-order kinetics in the presence of excess 1,3,5-trimethoxybenzene. The observed

reaction rate constant is linearly correlated with the concentration of 1,3,5-trimethoxybenzene (Figure S13). The second-order rate constant for the second reaction process was estimated to be  $0.38 \pm 0.01 \text{ M}^{-1}\text{s}^{-1}$ . The activation parameters for the second reaction process were also determined from the Eyring plot with reaction rate constants ranging from –30 to –70 °C (Figures S13 and S14). The activation of enthalpy ( $\Delta H^\ddagger$ ) and the activation of entropy ( $\Delta S^\ddagger$ ) were estimated to be  $32.5 \pm 2.7 \text{ kJ}\cdot\text{M}^{-1}$  and  $-109.6 \pm 12.3 \text{ J}\cdot\text{M}^{-1}\cdot\text{K}^{-1}$ , respectively. The negative  $\Delta S^\ddagger$  value indicates an associative transition state. We also conducted kinetic study of **1** for various aromatic compounds at –40 °C (Figure S15), and the results are summarized in Table 1. Apparently, the reaction rate

**Table 1.** Second-Order Rate Constants for Substrate Chlorination by **1** at –40 °C

substrate	$E_{\text{ox}}^a$	$k_2 \text{ (M}^{-1} \text{ s}^{-1}\text{)}$
anisole	1.23 <sup>b</sup>	too slow
1,4-dimethoxybenzene	0.94	$(3.07 \pm 0.03) \times 10^{-4}$
1,3,5-trimethoxybenzene	1.14 <sup>c</sup>	$(3.77 \pm 0.01) \times 10^{-1}$
1,2,3,5-tetramethoxybenzene	0.68 <sup>c</sup>	$(6.91 \pm 0.08) \times 10^{-1}$
cyclohexene	1.48 <sup>d</sup>	$(1.76 \pm 0.06) \times 10^{-2}$

<sup>a</sup>The  $E_{\text{ox}}$  values shown with SCE and Ag/Ag<sup>+</sup> references are calibrated to be Fc/Fc<sup>+</sup> by subscribing 0.53 and 0.57 V, respectively. The  $E_{\text{ox}}$  values can shift depending on solvents and temperature. <sup>b</sup>In CH<sub>3</sub>CN, ref 21. <sup>c</sup>In CH<sub>2</sub>Cl<sub>2</sub>, ref 22. <sup>d</sup>In CH<sub>3</sub>CN, ref 23.

constant increases with an increase in the number of the methoxy groups on the aromatic ring. To examine the direct electron transfer between **1** and substrate in the rate-limiting step, we plotted the reaction rate constant over the one-electron oxidation potential ( $E_{\text{ox}}$ ) of substrate (Figure S16). A good correlation was not identified. All of the present data indicated that an electrophilic aromatic substitution of **1** may be involved in the rate-limiting step of the chlorination reaction. The reaction of **1** with cyclohexene may also be explained by an electrophilic addition to the C=C bond (Figure S17).

There have been several reports of chlorination reactions by metalloporphyrin complexes.<sup>17–20</sup> Dichloromanganese(IV) porphyrin was shown to effect chlorination reactions to olefins via a radical mechanism.<sup>18</sup> Participation of analogous iron complexes, such as (TPFP<sup>2+</sup>)Fe<sup>III</sup>(Cl)<sub>3</sub> and (TPFP<sup>+</sup>)Fe<sup>IV</sup>(Cl)<sub>3</sub>, in the present chlorination reactions is ruled out by the absence of *cis*-1,2-dichlorocyclohexane from cyclohexene. Oxomanganese(V) porphyrins were also capable of chlorination reactions with formation of hypochlorite.<sup>19</sup> Formation of a chlorinating agent by (TPFP<sup>+</sup>)Fe<sup>IV</sup>O(NO<sub>3</sub>), formed by the reverse reaction from **1**, is also ruled out by the absence of oxygenation products. In addition, independence of the reaction rate on the concentration of chloride ion supports that **1** chlorinates substrates.

**1** also reacts with excess chloride ion much faster than organic substrates. In fact, when excess TBACl is used to prepare **1** from (TPFP<sup>+</sup>)Fe<sup>IV</sup>O(NO<sub>3</sub>), **1** is not formed effectively. Moreover, when 50 equiv of TBACl is further added after formation of **1** at –90 °C, **1** decomposes to (TPFP)Fe<sup>III</sup>Cl within a few minutes. The reaction of **1** with excess chloride ion is expected to result in the formation of a chlorine molecule. To identify a chlorine molecule from this reaction, 1,3,5-trimethoxybenzene, anisole, and cyclohexene were added to the mixture after the reaction of **1** with excess chloride ion at –90 °C. After the mixture warmed to room

temperature, the reaction products were analyzed by GC-MS. The products and their yields are shown in Figure 2. The chlorination products are the same as the products from **1**. The ratio of the *p*- and *o*-chloroanisoles is different from the ratio formed from **1**, but close to the ratio obtained in chlorination reactions using chlorine as reported previously.<sup>17</sup> These results indicate that **1** can react with excess chloride ion to form a chlorine molecule and (TPFP)Fe<sup>III</sup>Cl.

The chlorination reactions induced by iron(III) *meso*-chloro-isoporphyrin complex could be expanded in the development of a catalytic chlorination reaction. When ozone gas is bubbled into a mixture of (TPFP)Fe<sup>III</sup>Cl ( $5.0 \times 10^{-4}$  M, 1 mol %), TFA (0.1 M), TBACl (0.05 M), and 1,3,5-trimethoxybenzene (0.05 M) in DCM at room temperature for 1.5 h, 1-chloro-2,4,6-trimethoxybenzene is produced in 16% yield (turnover number = 16).<sup>24</sup> Moreover, the same product is also produced in 85% yield (turnover number = 85) when an aqueous solution of hydrogen peroxide is vigorously stirred with a mixture of (TPFP)Fe<sup>III</sup>Cl ( $5.0 \times 10^{-4}$  M, 1 mol %), TFA (0.1 M), TBACl (0.05 M), and 1,3,5-trimethoxybenzene (0.05 M) in DCM at room temperature for 1 h.<sup>24</sup> Similar catalytic chlorination reactions with a heme thiolate complex have been reported by Woggon et al.,<sup>20</sup> who proposed the formation of hypochlorite as a chlorinating agent in a haloperoxidase reaction. This process seems not to be involved under our conditions because the formation of **1** is much faster than the reaction of (TPFP<sup>+</sup>)Fe<sup>IV</sup>O(NO<sub>3</sub>) with TBACl.<sup>17</sup> In addition, isoporphyrin could not be formed under their conditions because acetic acid was used as proton source. Further studies are needed to optimize the reaction conditions and to clarify the mechanism of the catalytic reactions.

In summary, this study demonstrates the conversion of oxoiron(IV) porphyrin  $\pi$ -cation radical to iron(III) *meso*-chloro-isoporphyrin in the presence of chloride ion and TFA. The iron(III) *meso*-chloro-isoporphyrin complex formed in this reaction is a reactive agent capable of chlorination of aromatic compounds and olefins.

## ■ ASSOCIATED CONTENT

### Supporting Information

Figure S1–S17, Table S1 and S2, and experimental details. This material is available free of charge via the Internet at <http://pubs.acs.org>.

## ■ AUTHOR INFORMATION

### Corresponding Author

hiro@ims.ac.jp

### Notes

The authors declare no competing financial interest.

## ■ ACKNOWLEDGMENTS

This study was supported by grants from JSPS (Grant-in-Aid for Science Research, Grant No. 22350030) and MEXT (Global COE Program).

## ■ REFERENCES

(1) (a) Ortiz de Montellano, P. R. *Cytochrome P450. Structure, Mechanism, and Biochemistry*, 2nd ed.; Plenum: New York, 1995. (b) Denisov, I. G.; Makris, T. M.; Sligar, S. G.; Schlichting, I. *Chem. Rev.* **2005**, *105*, 2253–2278. (c) Watanabe, Y.; Groves, J. T. In *The Enzymes*; Sigman, D. S., Ed.; Academic Press: New York, 1992; Vol. 20, pp 405–452. (d) Fujii, H. *Coord. Chem. Rev.* **2002**, *226*, 51–60.

(2) (a) Murakami, T.; Yamaguchi, K.; Watanabe, Y.; Morishima, I. *Bull. Chem. Soc. Jpn.* **1998**, *71*, 1343–1353. (b) Nanthankumar, A.; Goff, H. M. *J. Am. Chem. Soc.* **1990**, *112*, 4047–4049.

(3) (a) Groves, J. T.; Watanabe, Y. *J. Am. Chem. Soc.* **1988**, *110*, 8443–8452. (b) Mizutani, Y.; Watanabe, Y.; Kitagawa, T. *J. Am. Chem. Soc.* **1994**, *116*, 3439–3441.

(4) Tsurumaki, H.; Watanabe, Y.; Morishima, I. *J. Am. Chem. Soc.* **1993**, *115*, 11784–11788.

(5) (a) Gold, A.; Ivey, W.; Toney, G. E.; Sangaiah, R. *Inorg. Chem.* **1984**, *23*, 2932–2935. (b) Abhilash, G. J.; Bhuyan, J.; Singh, P.; Maji, S.; Pal, K.; Sarkar, S. *Inorg. Chem.* **2009**, *48*, 1790–1792. (c) Rachlewicz, K.; Latos-Grażyński, L. *Inorg. Chem.* **1995**, *34*, 718–727.

(6) Woodward, R. B. *Pure Appl. Chem.* **1961**, *2*, 383–404.

(7) Dolphin, D.; Felton, R. H.; Borg, D. C.; Fajer, J. *J. Am. Chem. Soc.* **1970**, *92*, 743–745.

(8) Dinello, R. K.; Rousseau, K.; Dolphin, D. *Ann. N.Y. Acad. Sci.* **1975**, *244*, 94–106.

(9) (a) Davydov, R.; Matsui, T.; Fujii, H.; Ikeda-Saito, M.; Hoffman, B. M. *J. Am. Chem. Soc.* **2003**, *125*, 16340–16346. (b) Evans, J. P.; Niemez, F.; Buldain, G.; Ortiz de Montellano, P. *J. Biol. Chem.* **2008**, *283*, 19530–19539.

(10) (a) Wiseman, J. S.; Nichols, J. S.; Kolpak, M. X. *J. Biol. Chem.* **1982**, *257*, 6328–6332. (b) Ator, M. A.; David, S. K.; Ortiz de Montellano, P. *J. Biol. Chem.* **1989**, *264*, 9250–9257.

(11) Choe, Y. S.; Ortiz de Montellano, P. *J. Biol. Chem.* **1991**, *266*, 8623–8530.

(12) Raner, G. M.; Hatchell, J. A.; Dixon, M. U.; Joy, T. L.; Haddy, A. E.; Johnston, E. R. *Biochemistry* **2002**, *41*, 9601–9610.

(13) Takahashi, A.; Kurahashi, T.; Fujii, H. *Inorg. Chem.* **2009**, *48*, 2614–2615.

(14) (a) Schmidt, E. S.; Bruice, T. C.; Brown, R. S.; Wilkins, C. L. *Inorg. Chem.* **1986**, *25*, 4799–4780. (b) Lee, W. A.; Bruice, T. *Inorg. Chem.* **1986**, *25*, 131–135. (c) Mwakwari, C.; Fronczek, F. R.; Smith, K. M. *Chem. Commun.* **2007**, 2258–2260. (d) Bhuyan, J.; Sarkar, S. *Chem.—Eur. J.* **2010**, *16*, 10649–10652.

(15) Fujii, H. *Chem. Lett.* **1994**, 1491–1494.

(16) Brown, F. S.; Hager, L. P. *J. Am. Chem. Soc.* **1967**, *89*, 719–720.

(17) Cong, Z.; Kurahashi, T.; Fujii, H. *Angew. Chem., Int. Ed.* **2011**, *50*, 9935–9939.

(18) Kaustov, L.; Tal, M. E.; Shames, A. I.; Gross, Z. *Inorg. Chem.* **1997**, *36*, 3503–3511.

(19) (a) Umile, T. P.; Wang, D.; Groves, J. T. *Inorg. Chem.* **2011**, *50*, 10353–10362. (b) Liu, W.; Groves, J. T. *J. Am. Chem. Soc.* **2010**, *132*, 12847–12849.

(20) (a) Wagenknecht, H.-A.; Woggon, W.-D. *Angew. Chem., Int. Ed.* **1997**, *36*, 390–392. (b) Wagenknecht, H.-A.; Claude, C.; Woggon, W.-D. *Helv. Chim. Acta* **1998**, *81*, 1506–1520. (c) Woggon, W.-D. *Acc. Chem. Res.* **2005**, *38*, 127–136.

(21) Zweig, A.; Hodgson, W. G.; Jura, W. H. *J. Am. Chem. Soc.* **1964**, *86*, 4124–29.

(22) Nakagaki, T.; Shin-ichiro, K.; Harano, A.; Shinmyozu, T. *Tetrahedron* **2010**, *66*, 976–985.

(23) Fata, G.; Fleischmann, M.; Pletcher, D. *J. Electroanal. Chem.* **1970**, *25*, 455–459.

(24) The blank experiments, (TPFP)Fe<sup>III</sup>Cl ( $1.0 \times 10^{-3}$  M) in the presence of TBACl (0.05 M), TFA (0.1 M), and 1,3,5-trimethoxybenzene (0.05 M), formed 1-chloro-2,4,6-trimethoxybenzene in 0.1% yield (turnover number = 0.1).